Published in Journal of Modern Optics 49, 11, 1801-1809, 2002
which should be used for any reference to this work

Low-data simulation of diffractive optical elements based on the zones geometry

OLIVIER RIPOLL, VILLE KETTUNEN and HANS PETER HERZIG

Institute of Microtechnology, University of Neuchatel, Breguet 2, Neuchatel CH-2000, Switzerland; e-mail: olivier.ripoll@unine.ch

Abstract. Design and simulation of two-dimensional diffractive optical elements are often limited by the amount of data required to represent the element in the computer's memory. We present a technique based on a geometrical description of the element, which requires fewer data than the traditional pixel description. Moreover, the element is being described more accurately and consequently the pixel-related artefacts are suppressed. This technique can be used for both periodic and non-periodic structures of large dimensions under Fraunhofer or Fresnel approximations. We apply the method to analysis of far-field beam-shaping elements and discuss possible extensions and refinements of the technique.

1. Introduction

The deflection of light by diffraction at grating structures provides an accurate and flexible way to control wavefronts. Therefore the beam shaping of laser sources is often realized by means of diffractive optical elements (DOEs) [1, 2]. Design, simulation or analysis of such elements often requires large memory capabilities, which become a critical issue if either the features become very small compared with the element size, or the element size itself is large compared with the optical wavelength.

The usual way of representing a DOE for computation and fabrication is to sample it on a two-dimensional grid, generating a pixelated description. This method is well adapted to computational algorithms such as fast Fourier transform but can be costly in data size requirements. Moreover, many DOEs, especially the family of phase zone plates [3, 4], are not optimally described by a pixel representation, in terms of both accuracy and amount of data. An optimal technique could use the closed regions composing the DOE function as a way to describe it more exactly and with the minimum data. However, the simulation technique would have to take this description directly into account in order not to simply displace the problem.

For rotationally symmetric DOEs, such as simple Fresnel zone plates, one can use Bessel functions to calculate effectively the diffraction pattern of the element [5]. However, this possibility is very limited in practice. Formulae for Fraunhofer diffraction at arbitrarily shaped apertures also exist [6], but in practice they are computationally inefficient in all but the simplest cases. We present here a

technique that takes advantage of the DOE geometry, allowing the simulation of large elements with small features without any symmetry requirements. This technique not only drastically lowers the amount of data necessary for the computation but also is less sensitive to systematic errors compared with the classical two-dimensional sampling.

In section 2, we shall present the principles of the technique. We shall then tackle the many interests that arise from this description in terms of computation capabilities, accuracy and interaction with mask design. Section 4 will illustrate these interests with some simulations and experiments. Finally, we shall discuss the limitations and the possible extensions of this technique in section 5.

2. Basic principle

The basic principle of the technique is that the two directions of the space (x and y) are not treated equally. This is similar to the central slice theorem illustrated in figure 1, which states that the distribution along the central line at an angle θ of the two-dimensional Fourier transform of the function $f(x, y)$ is equal to the one-dimensional Fourier transform of the projection of $f(x, y)$ on the axis defining the central line (axis at angle θ) [7, 8]. While the classical computation is based on two successive Fourier transforms (through a fast Fourier transform (FFT) algorithm), first in the x direction, then in the y direction, the central slice theorem replaces the first Fourier transform by a projection (also called the Radon transform). Our technique, although derived from the central slice theorem, is not limited to central lines. Also, we can use propagation kernels other than the Fourier transform, as we shall discuss later.

For simplicity, we shall restrict our explanation to elements with closed regions of constant complex amplitude, under a uniform normally incident illumination. It is important to note that this limitation is not tied to the technique itself. Let us consider a closed region in the DOE plane of constant complex transmission C, as shown in figure 2 (a). The contour of this region can be decomposed between the

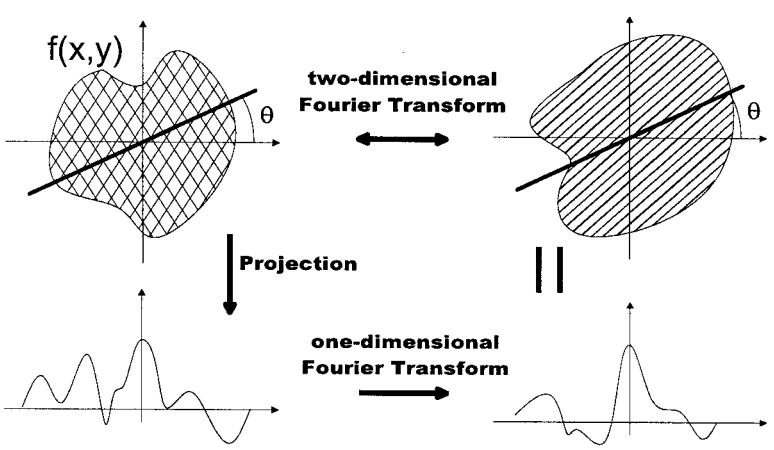

Figure 1. Principle of the central slice theorem. The value on a radial line at angle θ of the two-dimensional Fourier transform of $f(x, y)$ is equal to the one-dimensional Fourier transform of the projection at angle θ.

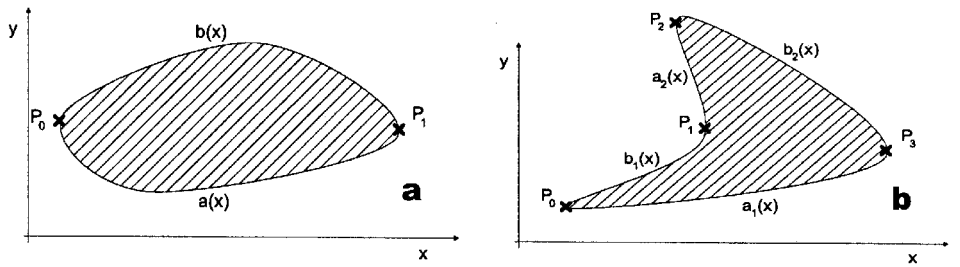

Figure 2. Description of a closed region in terms of upper and lower boundaries. (*a*) The boundaries are uniquely defined between points P_0 and P_1. (*b*) A closed contour can always be expressed as a set of upper and lower boundaries.

upper boundary $b(x)$ and the lower boundary $a(x)$. If the contour presents several upper boundaries and several lower boundaries as in figure 2 (*b*), it is easy to extend the following technique to take this property into account by decomposing the contour as a set of lower and upper partial boundaries associated end to end. Thus we can without loss of generality suppose the boundaries to be unique as in figure 2 (*a*).

In Fourier optics, the far-field light distribution $U'(u, v)$ is expressed as the Fourier transform of the input light field $U_{\text{in}}(x, y) = 1$ multiplied by the complex transmission function $t(x, y)$ as in

$$U'(u,v) = \int\int_{-\infty}^{\infty} U_{\text{in}}(x,y)t(x,y)\exp[-2i\pi(ux+vy)]\,dx\,dy. \tag{1}$$

For the previous shape delimited by $a(x)$ and $b(x)$, this can be expressed as the one-dimensional Fourier transform of $f_v(x)$, the projection of the region of complex amplitude C multiplied by a phase factor depending on the Fourier space coordinate v. Thus equation (1) can be written as

$$\begin{aligned} U'(u,v) &= \int_{-\infty}^{\infty} \left(\int_{a(x)}^{b(x)} C\exp(-2i\pi yv)\,dy \right) \exp(-2i\pi ux)\,dx \\ &= \int_{-\infty}^{\infty} f_v(x)\exp(-2i\pi ux)\,dx. \end{aligned} \tag{2}$$

Equation (2) reduces the two-dimensional Fourier transform to a one-dimensional Fourier transform, at the expense of being able to compute $f_v(x)$. For our region, this is simply given by

$$f_v(x) = \begin{cases} \dfrac{C}{2i\pi v}\{\exp[-2i\pi va(x)] - \exp[-2i\pi vb(x)]\}, & v \neq 0, \\ C[b(x) - a(x)] & v = 0. \end{cases} \tag{3}$$

Note that the case $v = 0$ is the expression of the central slice theorem. We have reduced our two-dimensional computation based on a large set of sampling points to a one-dimensional Fourier transform based on the knowledge of the boundaries of every closed region of the DOE, together with its complex transmission. This one-dimensional Fourier transform can be computed with the traditional FFT algorithm.

A closer look to the technique shows that it relies on the possibility of computing $f_v(x)$, which depends on the propagation and the closed-region decomposition of the input field. The propagation is responsible for the exponential term; the closed region decomposition contributes to the rest (in our simple case, just a constant term). This leads us to consider eventual limitations and extensions of the technique. A linearly blazed profile or an obliquely incident input wave, that is cases where the complex transmission C is not constant inside the considered closed region, will result in small changes in equations (2) and (3), due to an additional phase term of degree 1 in x and/or y. Switching to Fresnel diffraction will change the function of y in the complex exponential to a second-degree function. The resulting integral can still be computed. For a constant-valued region, it requires the use of the Fresnel integrals, or the complex error function $w(x)$, which can be obtained either through tabulated rational series [9] or through the algorithm presented by Weideman [10].

3. Comparison with the pixel-based approach

There are many advantages in using this closed-region description of the DOE. The main advantage is the drastic reduction in the data stored for the computation. The classical two-dimensional description uses a matrix whose size evolves as $\mathcal{O}(N^2)$, where N is the number of sampling points used in one direction, related to the resolution of the sampling. Our technique only requires the storage of the DOE pattern as a set of primitives, resulting in a nearly negligible amount of data. Furthermore the amount of data is independent of the resolution. For the computation to be sped up, the values of the upper and lower boundaries may be calculated and stored (note that this is not mandatory), leading to a data amount evolving as $\mathcal{O}(N)$. Increasing the resolution, or adding zeros (zero padding) around the DOE to avoid aliasing effects will not result in the generation of large data sets.

Another difference lies in the accuracy of the description. The two-dimensional sampling has a limit on how thin details can be represented. Typically, the sampling size defines a pixel that approximates the DOE ideal contour. If the DOE is of 'computer generated hologram (CGH) type' (e.g. a Dammann grating), whose design is directly based on a sampled description, no error is introduced. On the other hand, if the DOE is of, for example, a phase zone plate family with smooth contours, two situations are possible. Firstly, the pixelation (or tessellation) is present in both the simulation and the fabricated element and some artefacts might occur in the resulting far field. Alternatively, if the fabricated DOE's closed regions are smooth, then the pixelated simulation might be inaccurate. A typical artefact that can arise from a two-dimensional sampling of a DOE is the presence of a moiré-like effect generating parasite low frequencies. On the other hand, a description using closed contours is completely accurate for both types of DOE (pixel based and zone plates).

An interesting feature is also the possibility to calculate only the desired parts of the far field. The classical approach based on a two-dimensional FFT computes the whole output field while, in many cases, only a small part is of interest (e.g. the measurement of some aperture of a beam shaper, or scans on fan-out orders to measure respective intensities).

Finally, a very practical bonus of the shape description emerges when fabricating the DOE. From the shapes, it is easier to obtain optimal layout files used in, for

example, fabrication of lithography masks (generally Caltech intermediate format (CIF) or Calma GDS II (GDS) formats), since these file formats themselves are primitive based (mainly polygons for the CIF format).

4. Results

We performed some comparison between simulations and measurements to test the accuracy of the technique as a design tool. The design task was to compute a DOE used for beam shaping. Illuminated by some input wave, the aim is to redistribute the light in a specified far-field pattern. We designed far-field beam shapers for visible (633 nm) and ultraviolet light (248 nm). Some were binary, and some multilevel. The typical aperture angles of such beam shapers are about $\pm 1^{\circ}$.

In our implementation, we use various primitives for describing the DOE regions. We currently have the possibility to choose lines, arcs of circles, arcs of ellipses and cubic Bézier curves, all these primitives being associated end to end to describe a whole contour. In the computation these primitives are converted into boundaries $a(x)$ and $b(x)$. The implemented set of primitives proved to be very versatile. We have been able to simulate Fresnel zone plates in circular, square, hexagonal or trapezoidal cells for application as aperture modulated diffusers (AMDs)[11] as well as more complicated phase zone plates based on non-rotationally symmetric regions. The implemented set of primitives even extends to simulation of some CGH-type designs whose structure presents a closed-region aspect.

Concerning the accuracy of the technique, the simulations have shown excellent agreement with experimental results. We were able to predict the full width at half maximum with an accuracy comparable with the measurement error in our experiments (around 1%). The intensity profile itself was also predicted with an excellent agreement, as shown in figures 3 (*a*) and (*b*). In the experimental measurements the illumination was done with an excimer laser and was incoherent and slightly divergent. This was simulated by convoluting the source intensity distribution in the far field with the intensity distribution generated by the diffuser. The DOE was composed of many AMDs tiled to fill the element plane. The simulation of the influence of the phase offset [3] was found to follow the measurements, as shown in figures 4 (*a*) and (*b*). The radii and width of the rings in the far field correspond to the simulation, and the overall brightness of the ring with respect to its neighbours is also accurately predicted. However, the detector pixel size has a convolution effect resulting in a loss of contrast for the thinnest rings (farthest from the centre). The high intensity central peak is due to fabrication error, mainly etch depth error, which was not taken into account in the simulation. In figure 4, the illumination is done with a coherent plane wave. The DOE is a set of adjacent hexagonal AMDs filling the element plane.

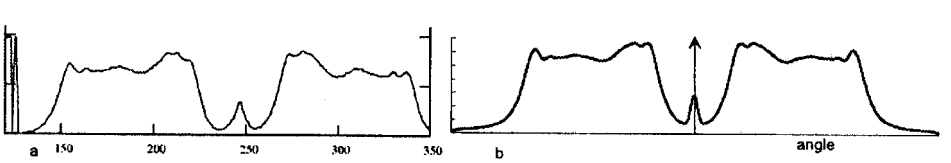

Figure 3. (*a*) Measured and (*b*) simulated far-field intensity distribution of a beam shaper with incoherent illumination.

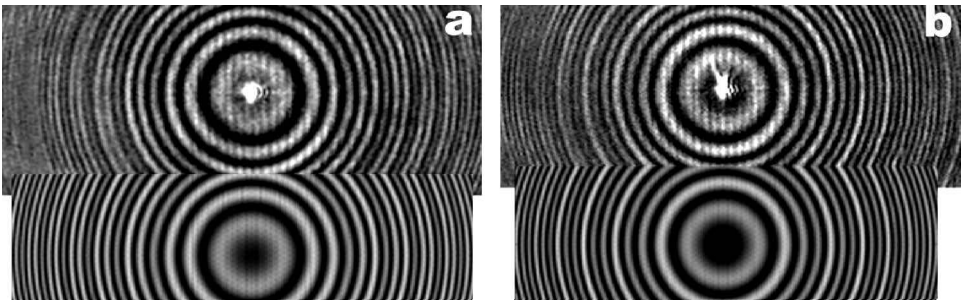

Figure 4. Magnification of the central area of the measured (top) and simulated (bottom) far-field of two hexagonal flat-top AMD beam shapers, illuminated by a coherent plane wave, where figures (*a*) and (*b*) differ in terms of their phase offset. The radii of the rings and their relative intensities are predicted with a good accuracy.

Another interest of the technique lies in the possibility of studying both periodic and aperiodic structures, as zero padding in one dimension is virtually costless. The oscillations present in the far field due to the tiling of the multiple diffusers can be studied and separated from those due to diffraction, as illustrated in figure 5. Figure 5 (*a*) shows the far field of a single hexagonal flat top beam shaper, and figure 5 (*b*) presents the far field of a group of several adjacent hexagonal cells. A slight smoothing has been applied to remove fast fluctuations and to keep only the envelope of the distribution. Three kinds of oscillation can be distinguished. At the centre, the oscillations are due to the digitization of the profile (i.e. a finite number of possible profile depths). They are mostly visible at the centre because it is the place where the dimensions of the annular zones of the DOE are the highest, and thus the error due to digitization is the largest. The edges of the DOE cell result in the boundary diffraction oscillations that can be seen on the sides of the hexagon. Finally, the periodicity results in interference effects that affect mainly the centre of the edges, as the comparison of the two simulations illustrates. It should be noted that this phenomenon is not a computational artefact but was also experimentally observed in measurements.

In terms of the amount of data, we also simulated two hexagonal flat-top beam shapers for 633 nm. The DOEs were 8 mm wide and some zero padding was used

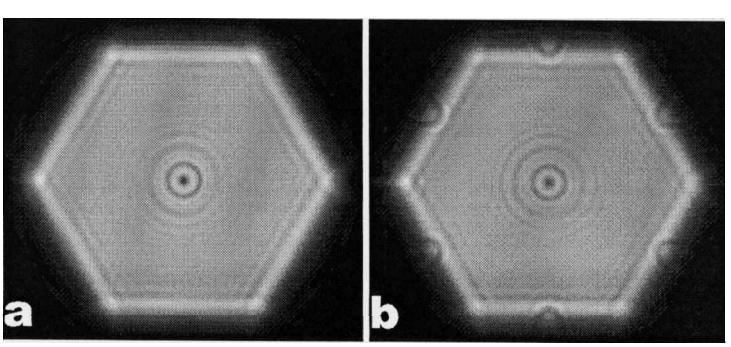

Figure 5. Simulated far field of an hexagonal flat-top plate made of a Fresnel zone plate: (*a*) single hexagonal cell; (*b*) a hexagonal array of adjacent cells.

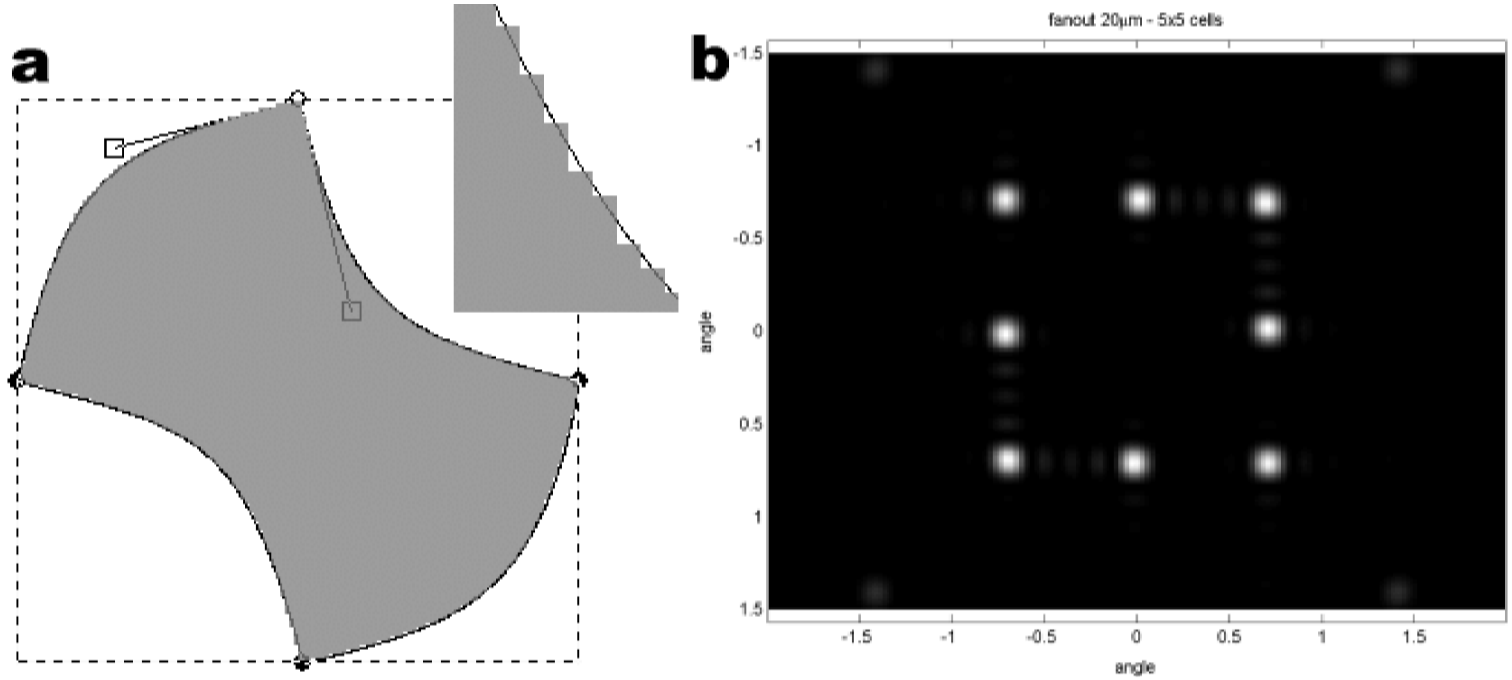

Figure 6. Curve approximation of a DOE designed by IFTA. (*a*) The original 128×128 matrix (the broken line represents its borders) is fitted by a piecewise cubic Bézier curve. A magnification of the fitting is shown in the top right corner. (*b*) The simulated far field of an element obtained by 5×5 tiling of the original cell.

around the elements, resulting in a final element size of 16 mm × 16 mm. One beam shaper was designed to generate a $\pm 1^{\circ}$ light distribution, and the other $\pm 5^{\circ}$. Both DOEs, if sampled on a 32 × 1024-point grid in each direction would require 16 Gbytes to be stored in Matlab. The computation itself requires at least double this memory (and three times in most cases). On the other hand, with the closed-region description, the computation of the first DOE, composed of 110 rings, would not require more than 30 Mbytes, while the computation of the second DOE, composed of 550 rings, needed only 150 Mbytes. This represents a reduction in the data requirements of 220–1000 times.

5. Discussion

The technique presented here has been explained with some restrictions for simplicity. We have already discussed the decomposition of complicated shapes into upper and lower boundaries necessary to the computation of equation (2). We have also assumed that the illumination was a normally incident plane wave. This may seem a strict limitation of the technique; however, an obliquely incident plane wave can be simulated through a change in the definition of $f_v(x)$ as given in equation (3). This change, the Fresnel propagation or a change in the profile of the regions of the phase zone plate to a blazed profile all lead to the use of the complex error function to compute equation (2), as already discussed in section 2.

The technique is not limited to DOE designed by ray-tracing or mapping techniques. Elements of grating type, designed by the iterative Fourier transform algorithm (IFTA) [12], often also exhibit closed regions of constant complex amplitude and thus are well suited to a description in terms of boundaries, as illustrated in figure 6 (*a*). In the considered example a basic cell of 128 × 128 pixels was described as a set of four Bézier cubic curves, presenting a smoother boundary [13]. This is illustrated by the magnification at the top right corner of figure 6 (*a*). The resulting far field of an element obtained by 5 × 5 tiling of this cell is given in figure 6 (*b*). An interesting point regarding this example is the low number of parameters used in the description. When symmetry considerations are taken into account, only three pairs of points are free for the whole shape, that is six parameters. One could imagine using this property to find high-resolution designs by refining a low-resolution solution obtained using IFTA through a simple parametric optimization step. Such a refinement could be beneficial in terms of both diffraction efficiency and stray light, as shown in [14]. We plan to investigate this possibility in the future.

In the previous sections, discussion was limited to cases where the thin element approximation was used to model the grating response. Thus the presented technique shares the limitations of other approaches based on this approximation and is not well suited to deep elements or gratings in the resonance domain. However, the presented method can be extended to the non-paraxial domain by incorporating the recently introduced step transition perturbation approach [15, 16]. In such an implementation the approach presented here would be accompanied by an additional step (or, alternatively, a modified diffraction kernel) where the existing description of the basic shapes making up the element would be used to calculate the field perturbations associated with the vertical profile transitions in the element according to the principles outlined in [16]. We expect such a method

to be an extremely powerful tool for the analysis and design of non-paraxial beam-shaping elements and intend to investigate this further in the future.

6. Conclusions

We have presented a computational technique well suited to the simulation of phase zone plates. Its main characteristic is the low amount of data required. This technique can be used for regions of very general contour, under both Fraunhofer and Fresnel approximations, and for DOE that present no symmetry.

We demonstrated that this technique really extends the size of the simulated DOE and gives results similar to classical Fourier computation, while requiring far fewer data to be stored during the computation. This technique was compared with measurements obtained from different fabricated elements and shows an excellent accuracy.

We discussed the possibility of extending this technique to other types of profile, for example cases where the surface profile is not constant, as well as to other diffraction kernels.

Acknowledgments

We wish to acknowledge Colibrys SA for financial support. We are grateful to Philippe Regnault and Felix Rudolf for some of the element characterizations as well as for fruitful discussions.

References

[1] Herzig, H. P. (editor), 1997, *Micro-optics: Elements, Systems and Applications* (London: Taylor & Francis), chapter I.
[2] Turunen, J., and Wyrowski, F. (editors), 1997, *Diffractive Optics for Industrial and Commercial Applications* (Berlin: Wiley–VCH,), chapter VI.
[3] Singer, W., Herzig H. P., Kuittinen, M., Piper, E., and Wangler, J., 1996, *Opt. Engng* **35,** 2779.
[4] Ross, I. N., Pepler, D. A., and Danson, C. N., 1995, *Optics Commun.*, **116,** 55.
[5] Goodman, J. W., 1968, *Introduction To Fourier Optics* (New York: McGraw-Hill), section 4.
[6] Komrska, J., 1982, *J. opt. Soc. Am.*, **72,** 1382.
[7] Gindi, G. R., and Gmitro, A. F., 1984, *Opt. Engng*, **23,** 499.
[8] Fraser, D., Hunt, B. R., and Su, J. C., 1985, *Opt. Engng*, **24,** 298.
[9] Abramovitz, M., and Stegun, I. A., 1972, *Handbook of Mathematical Functions* (New York: Dover Publications), section 7.
[10] Weideman, J. A. C., 1994, *SIAM J. numer. Anal.*, **31,** 1497.
[11] Herzig, H. P., and Kipfer, P., 1999, *International Trends in Optics and Photonics*, edited by T. Asakura (Berlin: Springer), p. 247.
[12] Fienup, J. R., 1982, *Appl. Optics*, **21,** 2758.
[13] Shao, L., and Zhou, H., 1996, *Graphical Models Image Processing*, **58,** 223.
[14] Schwarzer, H., Teiwes, S., and Wyrowski, F., 1997, in *Proceedings of the EOS Topical Meeting on Diffractive Optics*, EOS Technical Digest, Vol. 12, edited by J. Turunen J. and F. Wyrowski (Savonlinna, Finland), p. 20.
[15] Kettunen, V., Kuittinen, M., and Turunen, J. , *2001, J. opt. Soc. Am.* A, **18,** 1257.
[16] Vallius, T., Kettunen, V., Kuittinen, M., and Turunen, J., 2001, *J. mod. Optics*, **48,** 1195.